Advanced Droop Control Scheme in Multi-terminal DC Transmission Systems

Yanbo Che[†], Jinhuan Zhou*, Wenxun Li*, Jiebei Zhu** and Chao Hong***

Abstract – Droop control schemes have been widely employed in the control strategies for Multi-Terminal Direct Current (MTDC) system for its high reliability. Under the conventional DC voltage-active power droop control, the droop slope applies a proportional relationship between DC voltage error and active power error for power sharing. Due to the existence of DC network impedance and renewable resource fluctuation, there is inevitably a DC voltage deviation from the droop characteristic, which in turn results in inaccurate control of converter's power. To tackle this issue, a piecewise droop control with DC voltage dead band or active power dead band is implemented into controller design. Besides, an advanced droop control scheme with versatile function is proposed, which enables the converter to regulate DC voltage and AC voltage, control active and reactive power, get participated into frequency control, and feed passive network. The effectiveness of the proposed control method has been verified by simulation results.

Keywords: VSC, MTDC, Droop control, Power fluctuation, Frequency regulation, Dead band.

1. Introduction

High Voltage Direct Current (HVDC) transmission system has been identified as one of an ideal technology for bulk power transmission over long distances compared to traditional AC transmission systems due to a number of advantages [1]. As a key element of HVDC transmissions, power electronic converters in early-stage are based on Current Source Converter (CSC). CSC-HVDC usually uses series- or parallel-connected thyristors as basic switches, which requires an external voltage source for commutation [2]. With the development of fully-controlled power electronics, like Insulate Gate Bipolar Transistors (IGBT), Voltage Source Converter based HVDC (VSC-HVDC) systems exhibit a number of advantages over classical CSC-HVDC systems. By the fast acting Pulse Width Modulation (PWM) techniques, VSC-HVDC is able to control active and reactive power independently, feed weak AC systems with less risk of commutation failures and provide black start capability. VSC-HVDC can also change and reverse the DC network power flow instantly without changing DC voltage polarity [3].

The DC network connected with more than two converter terminals is referred to as a Multi-Terminal Direct Current (MTDC) system. MTDC networks have

been proposed to interconnect asynchronous AC systems. Terminals are usually connected in parallel with radial, ring, or meshed topology. VSC-MTDC, also known as a "DC super-grid" is deemed as a promising solution to the integration of large-scale renewable energies such as wind plants and photovoltaic (PV) power generations [2]. There has been a pan-Europe MTDC proposal which aims to collect wind power from the North Sea and interconnects with adjacent countries such as United Kingdom, Germany, Norway and Denmark for electricity trading [4]. China has commissioned two VSC based MTDC offshore applications: a three-terminal DC system with nominal DC voltage of ±160kV commissioned in Nan'ao island in 2013 [5], and a five-terminal DC system with nominal DC voltage of ±200kV commissioned in Zhoushan in 2014 [6].

MTDC improves reliability and flexibility in system operation by involving more terminals into power allocation; the control complexity is conversely increased. Master-slave control is the extension of coordination control in point-to-point HVDC scheme. Two-terminal HVDC assigns one VSC at power control mode and the other one at DC voltage regulation mode. Similarly, for MTDC system, the terminal controlling DC voltage is known as the master terminal, while the other terminals operate under current or power control. Master terminal is a slack bus to balance total power inputs and outputs in the MTDC network. Master-slave control is subject to the danger of DC voltage instability under circumstances of losing terminals or abrupt power change [7]. A fast communication may help to relieve master terminal's burden and improve operation reliability by rescheduling the power order or reassigning master terminal [8]. But

---

† Corresponding Author: Key Laboratory of Smart Grid of Ministry of Education, Tianjin University, China. (lab538@163.com)
* Key Laboratory of Smart Grid of Ministry of Education, Tianjin University, China. (uestc_zjh@163.com, lwx2015@tju.edu.cn)
** Department of System Operators, National Grid plc, UK. (zhujiebei@hotmail.com)
*** State Key Laboratory of HVDC, Electric Power Research Institute, CSG, China. (hongchao@csg.cn)

communication latency may have a negative effect on system's fast response.

Two basic communication-free methods were historically reported to meet stable operation of MTDC: voltage margin control [9] and voltage droop control (also known as slope control) [7]. The voltage margin control, built on the basic principle of master-slave control, enables the switchover of the master terminal from one to another when the prevailing master's power capability is exceeded while allowing different levels of DC voltage margins. However, the quantity of terminal in MTDC system is restricted by limited voltage margin. Voltage droop control employs droop characteristics for terminals [7], which is designed according to the voltage limit of system and power rating of converter [10]. Under the voltage droop control scheme, the operational DC voltage for a terminal is controlled to vary along with its local droop characteristic to allow power change. It can make the lost power properly shared amongst the different droop controlled converters after the outage of a converter, which makes the voltage droop control more suitable for large DC grids[11]. This method involves more terminals in DC voltage control and power sharing without reliance on fast communication, which may show higher reliability than master-slave control [12]. However, compared to margin control, voltage droop control involves very complex droop control characteristics in accurate power flow control [10]. To ensure the coordinated operation of MTDC system, the droop ratio and dead band should be selected to alleviate the impact of transient events on the operating points of converter stations [13]. Under the circumstances of renewable power fluctuation as exported by the MTDC network, DC voltage fluctuation are naturally resulted to disturb the droop characteristic which is designed mainly for steady state. This causes the power errors for the terminals in MTDC system. Additionally, as large-scale integration of renewable energy negatively impacts the behavior of grid frequency, effective control scheme must be introduced to reduce the frequency deviation [14].

To enhance power flow control in MTDC and exert flexible characteristic of the converter, this paper proposes an advanced droop control scheme with the detailed design for the controllers. For accurate power flow control, droop control with voltage dead band and droop control with power dead band are applied to the master station and slave stations respectively. Frequency measurement is introduced into the controller to damp oscillation in the system. The AC voltage control is also embedded into controller design.

The remaining of this paper is organized as follows: in Section 2, voltage droop control is introduced and power error caused by system losses and renewable energy fluctuation is discussed. In section 3, droop control is modified with voltage dead band and power dead band to reduce power fluctuation of the converter. The advanced droop control is proposed by integrating basic droop control, frequency regulation control and AC voltage

control. The dead band can be added to achieve piecewise droop control. In Section 4, the performance of the advanced droop control is tested by an MTDC model simulated in MATLAB/Simulink. The conclusion is drawn in Section 5.

2. Voltage Droop Control of VSC

The complete configuration of inner and outer controllers for a VSC is depicted in Fig. 1. To facilitate VSC power regulation, the VSC three-phase voltage and current at Point of Common Coupling (PCC) are transformed into d-q framework. When the VSC is operated in grid connection mode, the angular position θ for d-q transformation is derived in real time from Phase Locked Loop (PLL). When VSC is operated in islanded mode, θ is defined by integrating $2\pi f$ (f is the desired frequency of the system, e.g. 50Hz) without PLL. For independent active and reactive power control as well as AC and DC voltage regulation, the dedicated outer controllers generate current references by the PI controller as inputs to the inner current loop. By taking account of the electrical characteristics of the VSC, AC reactor and transformer, the inner current controller computes the desired converter-side voltage reference for the VSC's PWM [15]. For the protection of converter, current and voltage limits are embedded into local controller design, to ensure converter operation in a
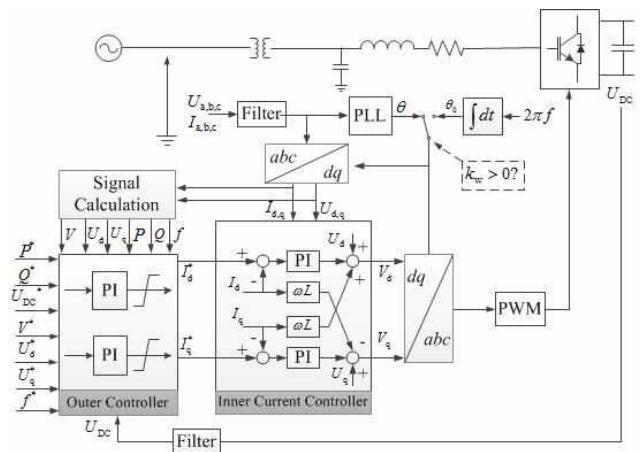

Fig. 1. Control block diagram for VSC

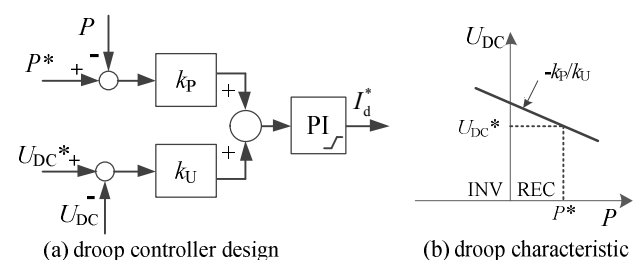(a) droop controller design   (b) droop characteristic

Fig. 2. Droop controller design and its characteristic

safe zone.

In the following contents, the outer controller to generate d-axis reference current is taken as the example for analysis. DC voltage-active power droop control is the most commonly used outer controller. The droop controller design and its characteristic are shown in Fig. 2. Positive power is defined as flowing into DC grid (i.e. converter in rectifying mode).

The input of outer controller is given by

$$e = k_{\mathrm{P}}(P^* - P) + k_{\mathrm{U}}(U_{\mathrm{DC}}^* - U_{\mathrm{DC}}) \qquad (1)$$

where P^*, P, U_{DC}^* and U_{DC} are the reference and measured active power and DC voltage of converter, k_{P} and k_{U} are the gains of power error and voltage error.

The input error is regulated to zero by dynamically adjusting of PI controller, so VSC's active power in steady state satisfies:

$$P = P^* + \frac{k_{\mathrm{U}}}{k_{\mathrm{P}}}(U_{\mathrm{DC}}^* - U_{\mathrm{DC}}) \qquad (2)$$

VSC's active power is related to its locally measured DC voltage. Under circumstances where the power surplus in the MTDC network results in an overall DC grid voltage rise, the DC voltage for all the VSCs with droop control will slide overall following the droop characteristics to reduce input power or increase output power to suppress voltage rise. More than one VSC can take part in this process, while there is no conflict in regulating DC grid voltage.

Voltage droop control shows high reliability for coordination control among VSCs. However, VSC's active power is vulnerable to disturbance of DC voltage, because of the influence of transmission impedance and power fluctuation from renewable resources.

DC voltages at different VSC terminals, as indicators for DC power balance, differ according to the directions of power flows via the MTDC network. The converters inputting power into DC grid tend to have higher DC voltage than the power outputting ones. While the operating point of the converter has deviated, the VSCs under individual droop characteristics are self-adjusting according to locally measured DC voltage in a relatively uncoordinated manner. Due to the proportional nature of droop control, as explained in function (1), there is a power error as long as a voltage deviation exists.

The influence of transmission impedance can be eliminated by setting different reference operating points for different VSCs according to power flow analysis results. However, the intermittent renewable resources bring in DC grid voltage fluctuation, which cannot be eliminated with the aid of power flow analysis. The impacts from renewable resource fluctuation need to be taken into consideration in designing droop controller.

3. Advanced Droop Control

3.1 Droop control with voltage dead band

Compared to the parallel voltage-power droop control, the proposed droop control embeds a constant power section onto the droop control to achieve accurate power flow control. In the dead band, VSC operates in constant power control mode. Out of the dead band, VSC operates in droop control mode.

The controller design and characteristic of droop control with voltage dead band are shown in Fig. 3. A section of constant power control is incorporated into conventional droop characteristic. The droop characteristic is divided into two sections. The slopes are defined as

$$-\frac{k_{\mathrm{P1}}}{k_{\mathrm{U1}}} = -\frac{U_{\mathrm{DC\_max}} - (U_{\mathrm{DC}}^* + \mathrm{d}U_p)}{P^* - P_{\min}}$$
$$-\frac{k_{\mathrm{P2}}}{k_{\mathrm{U2}}} = -\frac{(U_{\mathrm{DC}}^* - \mathrm{d}U_n) - U_{\mathrm{DC\_min}}}{P_{\max} - P^*} \qquad (3)$$

where $U_{\mathrm{DC\_max}}$, $U_{\mathrm{DC\_min}}$, $P_{\max}$ and $P_{\min}$ are the upper and lower limit of system DC voltage and VSC's capacity, respectively, $\mathrm{d}U_p$ and $\mathrm{d}U_n$ are the upper and lower limit of voltage dead band.

3.2 Droop control with power dead band

Similarly, droop control with power dead band embeds a constant voltage section onto the droop control. In the dead band, VSC operates in constant voltage control. Out of the dead band, VSC operates in droop control.

The controller design and characteristic of droop control with power dead band are shown in Fig. 4. A section of
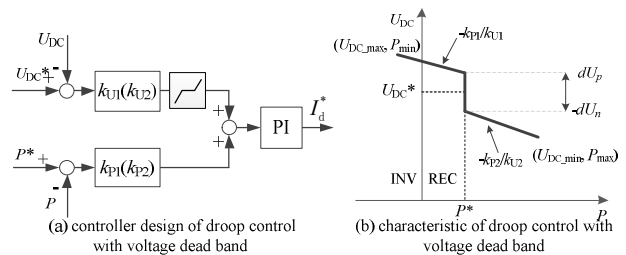

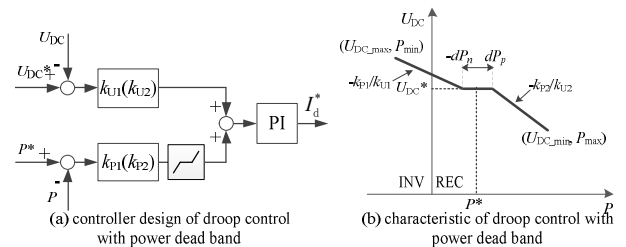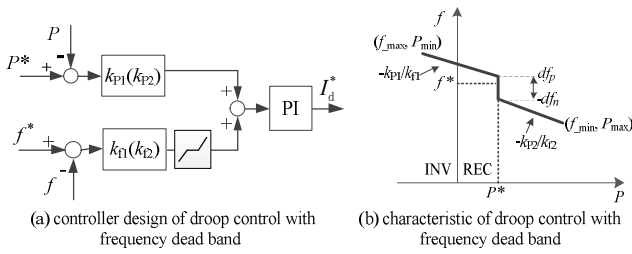**Fig. 3.** Droop control with voltage dead band

Fig. 4. Droop control with power dead band

(a) controller design of droop control with frequency dead band

(b) characteristic of droop control with frequency dead band

Fig. 5. Droop control with frequency dead band

constant voltage control is incorporated into conventional droop characteristic. The slopes of two droop section are defined as

$$-\frac{k_{P1}}{k_{U1}} = -\frac{U_{DC\_max} - U_{DC}^{*}}{P^{*} - dP_{n} - P_{min}}$$
$$-\frac{k_{P2}}{k_{U2}} = -\frac{U_{DC}^{*} - U_{DC\_min}}{P_{max} - (P^{*} + dP_{p})}$$

(4)

where dP_p and dP_n are the upper and lower limit of power dead band respectively.

3.3 Droop control with frequency dead band

When the capacity of VSC is large enough, it's possible for VSC to participate in frequency regulation in AC system. The frequency at PCC is measured and feedback to the controller, as shown in Fig. 5. A dead band is added to the frequency error, which means VSC is not involved in frequency regulation in normal states. It only takes effect when a large disturbance occurred with large frequency deviation detected.

The slopes of two droop section are defined as

$$-\frac{k_{P1}}{k_{f1}} = -\frac{f_{max} - (f^{*} + df_{p})}{P^{*} - P_{min}}$$
$$-\frac{k_{P2}}{k_{f2}} = -\frac{(f^{*} - df_{n}) - f_{min}}{P_{max} - P^{*}}$$

(5)

where f_{max} and f_{min} are the upper and lower limit of system frequency, df_p and df_n are the upper and lower limit of frequency dead band, and k_f is the gain of system frequency.

3.4 Advanced droop control

In order to combine the functionalities of different control modes, an advanced droop controller is proposed to enhance the control flexibility and versatility, as illustrated in Fig. 6. The explanations of different variables used in this paper are listed in Table 1. All the measurements are in per unit.

As shown in Fig. 6, in grid connection mode, a
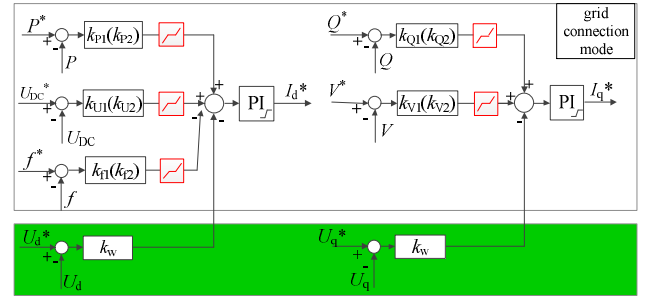
Fig. 6. Implementation of advanced droop control

Table 1. Meanings of the symbols

Items	Variables (in per unit)			
	measured values	reference values	errors	gains of errors
active power	P	P^{*}	eP	k_{P1}, k_{P2}
DC voltage	U_{DC}	U_{DC}^{*}	eU_{DC}	k_{U1}, k_{U2}
frequency	f	f^{*}	ef	k_{f1}, k_{f2}
reactive power	Q	Q^{*}	eQ	k_{Q1}, k_{Q2}
AC voltage magnitude	V	V	eV	k_{V1}, k_{V2}
AC voltage in d-axis	U_d	U_d^{*}	eU_d	k_w
AC voltage in q-axis	U_q	U_q^{*}	eU_q	k_w

All gains of errors are greater than or equal to 0.

generalized droop control is constructed by combining active measurements (DC voltage, active power and frequency) and reactive measurements (reactive power and AC voltage amplitude). Contrary to traditional droop control, the DC voltage, active power, reactive power and frequency can be controlled by setting different parameters of a single regulator. The complexity of the controller structure is reduced and it's more flexible to select control variables according to coordinated operation requirements. The dead band can be enabled to achieve piecewise droop control of converter. The reference operating point of VSC and upper and lower limit of the dead band need to be determined with the aid of power flow analysis while taking renewable resources fluctuation into consideration. In islanded mode, AC voltage at PCC is regulated to maintain stable to feed passive network.

For coordination control in parallel MTDC, DC voltage can only be controlled by one master terminal. So droop control with a section of constant DC voltage control can only be applied to one master station, while the other terminals' (slave terminals) control modes are not restricted.

4. Simulation Verifications and Discussions

4.1 System parameters

A five-terminal bipolar HVDC as shown in Fig. 7 is modeled in MATLAB/Simulink to test the proposed control methods. VSC1~3 are connected to three independent AC systems. The PV plant is connected to VSC4 to transmit solar power into DC grid. A passive load is connected to VSC5. The parameters of the system model are listed in
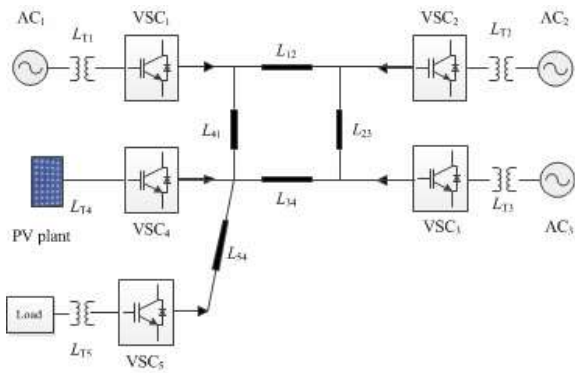
Fig. 7. Five-Terminal VSC-HVDC

Table 2. Parameters of the modeled system

Parameters		Values
Nominal Power		200 MVA
AC Nominal Voltage		110 kV/100 kV
DC Nominal Voltage		±100 kV
Phase Reactor L_T		47.7 mH
Line Resistance		0.015 Ω/km
Line length [L_{12}, L_{23}, L_{34}, L_{41}, L_{54}]		[180, 150, 230, 500, 200] km
	VSC1	[-100, 100] MVA
	VSC2	[0, 120] MVA
Converter Capacity	VSC3	[-120, 0] MVA
	VSC4	[0, 20] MVA
	VSC5	[-40, 0] MVA

Table 3. 5 modes in simulation

Mode	Power flow analysis	Renewable energy	Dead band
Scheme1	no	constant	no
Scheme2	with	constant	no
Scheme3	with	fluctuate	no
Scheme4	with	fluctuate	dead band 1
Scheme5	with	fluctuate	dead band 2

Table 2.

Versatile droop controller as mentioned above is implemented in VSC1~5. VSC1~3 are in grid connection mode, and VSC5 is in islanded mode. VSC1 is selected to be master terminal employing droop control with power dead band. VSC2~VSC3 are salve terminals employing droop control with voltage dead band and frequency dead band. VSC2 inputs 0.4pu constant power into the DC grid and VSC3 inputs 0.5pu constant power into AC grid. PV plant inputs maximum solar power to DC grid by VSC4. VSC5 supplies a passive network.

In order to verify the performance of advanced droop control strategy, 5 typical operation modes are selected from three aspects: a) whether the operation reference point is determined by power flow analysis, b) whether there is a fluctuation of renewable energy, c) whether there is a dead band. The 5 modes are listed in Table 3.

The fluctuation range of the output power of renewable energy is 0~0.1pu, and the average value is 0.05pu. According to the fluctuation range of renewable energy, an open source program for AC/DC power flow analysis,

Table 4. The results of power flow analysis

Initial parameters (pu)		Power flow analysis results (pu)	
PV minimum output power 0pu	$U_{dc1}=1.00000$ $\begin{bmatrix} P_2 \\ P_3 \\ P_4 \\ P_5 \end{bmatrix} = \begin{bmatrix} 0.4 \\ -0.5 \\ 0 \\ -0.2 \end{bmatrix}$	$P_1 = 0.322$ $\begin{bmatrix} U_{dc2} \\ U_{dc3} \\ U_{dc4} \end{bmatrix} = \begin{bmatrix} 0.9868 \\ 0.9851 \\ 0.9787 \end{bmatrix}$	
PV average output power 0.05pu	$U_{dc1}=1.00000$ $\begin{bmatrix} P_2 \\ P_3 \\ P_4 \\ P_5 \end{bmatrix} = \begin{bmatrix} 0.4 \\ -0.5 \\ 0.05 \\ -0.2 \end{bmatrix}$	$P_1 = 0.271$ $\begin{bmatrix} U_{dc2} \\ U_{dc3} \\ U_{dc4} \end{bmatrix} = \begin{bmatrix} 0.9974 \\ 0.9863 \\ 0.9807 \end{bmatrix}$	
PV maximum output power 0.1pu	$U_{dc1}=1.00000$ $\begin{bmatrix} P_2 \\ P_3 \\ P_4 \\ P_5 \end{bmatrix} = \begin{bmatrix} 0.4 \\ -0.5 \\ 0.1 \\ -0.2 \end{bmatrix}$	$P_1 = 0.220$ $\begin{bmatrix} U_{dc2} \\ U_{dc3} \\ U_{dc4} \end{bmatrix} = \begin{bmatrix} 0.9981 \\ 0.9875 \\ 0.9828 \end{bmatrix}$	

Table 5. The values of different dead band.

Dead band	VSC1	VSC2	VSC3
1	$\Delta P_{11}=0.051pu$	$\Delta U_{21}=0.0006pu$	$\Delta U_{31}=0.0012pu$
2	$\Delta P_{12}=0.100pu$	$\Delta U_{22}=0.0012pu$	$\Delta U_{32}=0.0024pu$

MATACDC [16], is employed in this paper to calculate power flow, and the results are shown in Table 4. The corresponding droop characteristics and dead band value are determined according to the results. The dead band values in scheme 4 and scheme 5 are shown in Table 5. Dead band 2 is larger than dead band 1.

4.2 Simulation results

4.2.1. Power Flow Control

(1) The Influence of System Transmission Loss
Two droop control schemes are implemented, including conventional droop control without and with power flow analysis. Assuming that the output power of PV system is 0.05pu. In scheme 1, the system loss is neglected, and the reference voltages of all VSCs are regarded as 1pu. In scheme 2, considering of the transmission line loss of the system, the reference operating points of VSCs are determined by power flow analysis as listed in Table 4(P_4=0.05).

The DC voltages of VSC1~5 in scheme 1 & 2 have been depicted in Fig. 8. In scheme 1, all of the DC voltages at five VSCs are deviated from the reference value (1pu). In scheme 2, the DC voltages are almost the same with the results in Table 4(P_4=0.05).

The power outputs of VSC1~5 in schemes 1 & 2 are depicted in Fig. 9. It's clear that there is a power error of VSC1~3 in steady state when the system losses are not considered in scheme 1. This error can be eliminated with the aid of power flow analysis. The power deviation is
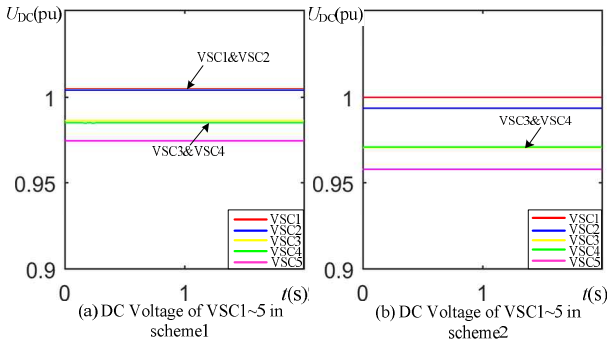
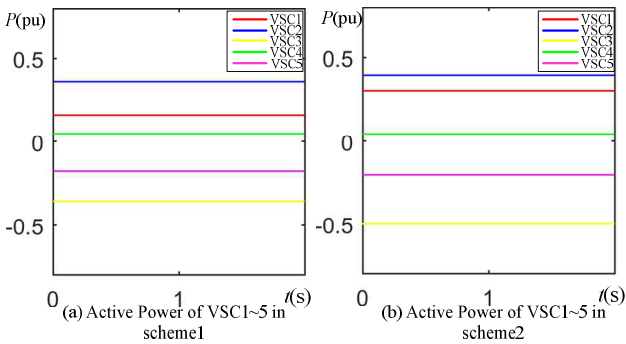**Fig. 8.** DC voltages of VSCs in scheme 1 & 2

Fig. 9. Power outputs of VSCs in scheme 1 & 2

greatly reduced, and steady state performance of the system is improved in scheme 2.

(2) The Influence of Renewable Energy Fluctuation

In order to test the effectiveness of the dead band on output power of VSCs, conventional droop control without the dead band (scheme 3) and the advanced droop control with different dead band (scheme 4 & 5) are simulated. The reference operating points are determined with power flow analysis. The average output power of PV system is 0.05pu. The reference operating points of VSC1~5 are listed in Table 4. The solar irradiance of PV plants in the simulation model is changed to simulate the fluctuation of atmosphere condition. The AC active power of each VSC in different schemes are compared in Fig. 10. The power output fluctuation of PV plant (Fig. 10(d)) leads to DC voltage fluctuation. As it can be observed, in scheme 3, the power outputs of VSCs with droop control are all affected by this fluctuation and the power fluctuation are shared by all VSCs. With the introduction of dead band, the power fluctuation is mainly balanced by the master terminal VSC1. The effectiveness of the slave converter station maintaining constant power output is better, when the dead band is larger. The powers of VSC2, VSC3 and VSC5 are almost kept constant in scheme 5, regardless of the DC voltage fluctuation. This indicates that the introduction of the dead band can effectively reduce the negative influence of renewable resource fluctuation.
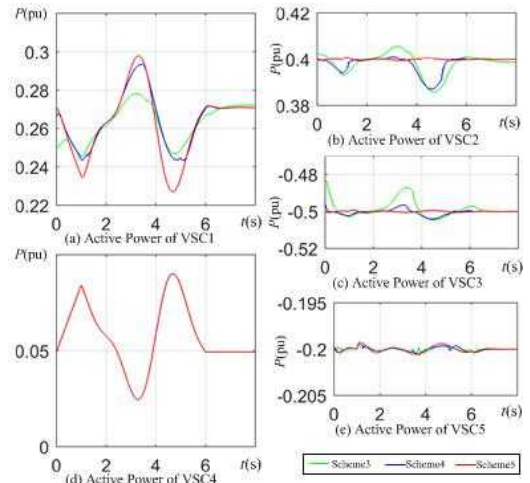

Fig. 10. Power outputs of VSCs in scheme 3 & 4
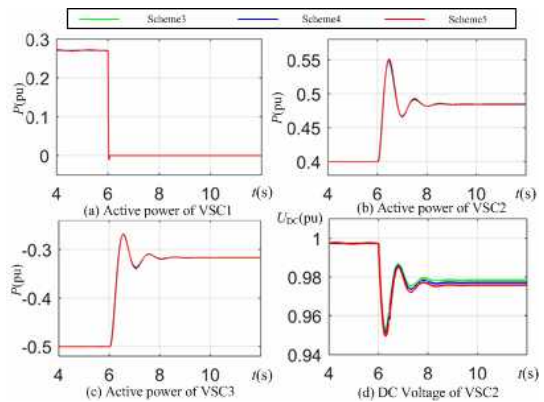

Fig. 11. Results of VSCs when VSC1 outage

(3) Converter Outage

This section aims at evaluating the transient performance of the proposed advanced droop-control strategy. The output power of PV system is 0.05pu. With the same initial condition, the master terminal VSC1 is cut off from DC grid at 6s adopting different control strategies. The DC voltages and power outputs of VSCs are shown in Fig11. The system can reach to a new steady state rapidly, and the power shortage is shared among VSCs using droop control. VSC2 increases input power and VSC3 reduces output power to stop DC voltage from falling. There are only slave terminals adopting voltage dead band in the MTDC system. Therefore, the voltage deviation is larger when the voltage dead band is larger (Fig. 11(d)).

Under the same initial conditions as described in the last case, the slave terminal VSC3 is cut off from DC grid at 6s. The results are shown in Fig. 12. VSC1 turns to be in inverter mode to maintain the DC voltage and balance the active power. The input power of VSC2 is also reduced. The introduction of dead band makes the droop characteristic more complex. The master station, VSC1, has high power flexibility due to the existence of the power
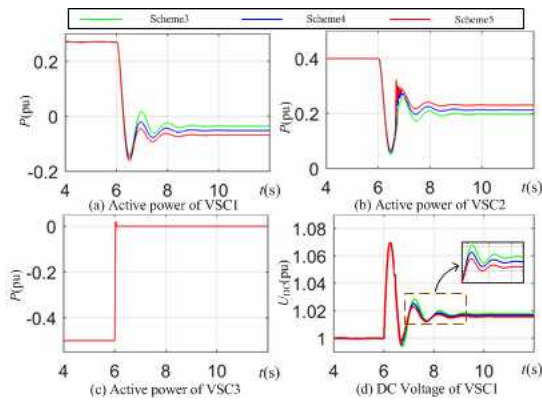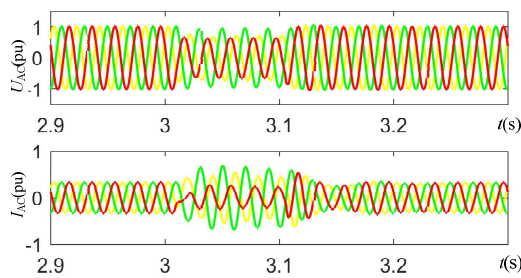
Fig. 12. Results of VSCs when VSC3 outage

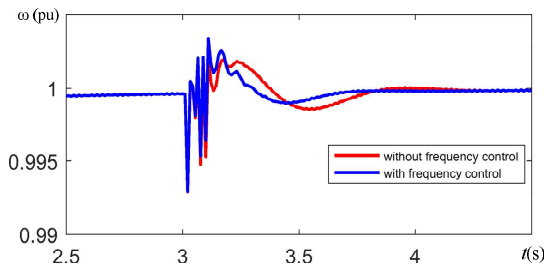**Fig. 13.** AC voltage and current of VSC2

Fig. 14. Rotor speed of generator I n AC system

Table 5 Dead band of frequency control

	VSC1	VSC2	VSC3
Frequency dead band	[-0.001, 0.001]	[-0.001, 0.001]	[-0.001, 0.001]

dead band. The voltage deviation is less when the dead band is larger (Fig. 12(d)). The power sharing of master station, VSC1, is larger with larger power dead band (Fig. 12(a)). The power sharing of slave station is less with larger voltage dead band (VSC2 in Fig. 12(b)).

4.2.2. Frequency Control

The results presented in 4.2.1 illustrate the effectiveness of the voltage dead band and the power dead band. The disturbance also significantly affects frequency behavior. The frequency control parameters of the advanced control strategy are listed in Table 5. A Single phase ground fault
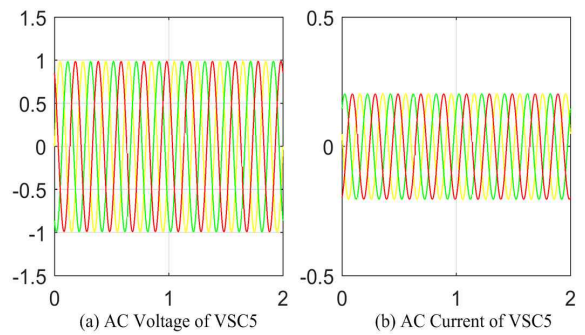

Fig. 15. AC voltage and current at PCC of VSC5

occurred in 3~3.1s in AC system 2. The AC voltage and current at PCC of VSC2 is shown in Fig. 13. The rotor speed of generator in AC system with and without frequency control is shown in Fig. 14. The frequency is more stable with VSC participate into frequency control.

4.2.3. AC Voltage Control

VSC5 is connected with a passive network, so AC voltage control is implemented in VSC5. The AC voltage and current at PCC of VSC5 is shown in Fig. 15, VSC5 inputs about 0.2pu power to the load.

5. Conclusion

This paper presents an advanced droop control scheme, which unifies different control mode of VSC. The droop characteristic is implemented among DC voltage, active power, frequency and d-axis voltage to generate the d-axis reference current. Droop control among reactive power, AC voltage magnitude and q-axis voltage are used to generate the q-axis reference current. According to power flow analysis, different reference operating points for different VSCs can be set to eliminate the influence of transmission impedance on MTDC power flow control. The dead band can be added to achieve piecewise droop control. It is shown by simulations that the introduction of the dead band can effectively improve the steady-state performance. In normal operation conditions, the power loss and the renewable fluctuation are mainly consumed by the master station. Furthermore, it is shown by simulations that the system can reach to a new steady state even one of the station in MTDC system is lost, which shows high reliability. VSC is able to exert its versatile function of DC voltage and active power control, frequency control, and AC voltage control with the proposed control scheme.

and Technology Project of China Southern Power Grid (CSGTRC-K163001).

References

[1] M. Araguees-Penalba, A. Egea-Alvarez, S. Galceran Arellano, and O. Gomis-Bellmunt, "Droop control for loss minimization in HVDC multi-terminal transmission systems for large offshore wind farms," *Electric Power Systems Research,* vol. 112, pp. 48-55, Jul 2014.

[2] B. Badrzadeh, "Power conversion systems for modern ac-dc power systems," *European Transactions on Electrical Power,* vol. 22, pp. 879-906, 2012.

[3] Yanbo Che, Wenxun Li, Xialin Li, et al, "An Improved Coordinated Control Strategy for PV System Integration with VSC-MVDC Technology," *Energies,* Vol. 10, pp. 1-14, 2017.

[4] *Friends of the Supergrid, Supergrid Phase 1.* Available: http://mainstreamdownloads.opendebate. co.uk/downloads/Supergrid-Phase-1-Final.pdf.

[5] H. Rao, "Architecture of Nan'ao multi-terminal VSC-HVDC system and its multi-functional control," *CSEE Journal of Power and Energy Systems,* vol. 1, pp. 9-18, 2015.

[6] M. A. Perez, S. Bernet, J. Rodriguez, S. Kouro, and R. Lizana, "Circuit Topologies, Modeling, Control Schemes, and Applications of Modular Multilevel Converters," *IEEE Transactions on Power Electronics,* vol. 30, pp. 4-17, Jan 2015.

[7] C. D. Barker and R. Whitehouse, "Autonomous converter control in a multi-terminal HVDC system," in *2010. ACDC. 9th IET International Conference on AC and DC Power Transmission*, 2010, pp. 1-5.

[8] J. Zhu, C. D. Booth, G. P. Adam, and A. J. Roscoe, "Coordinated direct current matching control strategy for multi-terminal DC transmission systems with integrated wind farms," *Electric Power Systems Research,* vol. 124, pp. 55-64, 7// 2015.

[9] T. Nakajima and S. Irokawa, "A control system for HVDC transmission by voltage sourced converters," in *1999 IEEE Power Engineering Society Summer Meeting*, 1999, pp. 1113-1119 vol. 2.

[10] R. S. Whitehouse, "Technical Challenges of Realising Multi-terminal Networking with VSC," *in Proceedings of the 2011-14th European Conference on Power Electronics and Applications (Epe 2011)*, 2011.

[11] Beerten J, Cole S, Belmans R. "Modeling of Multi-Terminal VSC HVDC Systems With Distributed DC Voltage Control," *IEEE Transactions on Power Systems*, vol. 29, pp. 34-42, 2013.

[12] T. M. Haileselassie and K. Uhlen, "Precise control of power flow in multiterminal VSC-HVDCs using DC voltage droop control," in *2012 IEEE Power and Energy Society General Meeting*, 2012, pp. 1-9.

[13] Li H, Liu C, Li G, et al. "An Enhanced DC Voltage Droop-Control for the VSC-HVDC Grid," *IEEE Transactions on Power Systems*, pp. (99):1-1, 2017.

[14] Silva B, Moreira C L, Seca L, et al. "Provision of Inertial and Primary Frequency Control Services Using Offshore Multiterminal HVDC Networks," *IEEE Transactions on Sustainable Energy*, vol. 3, pp. 800-808, 2012.

[15] L. Weixing and O. Boon-Teck, "Optimal acquisition and aggregation of offshore wind power by multi-terminal voltage-source HVDC," *IEEE Transactions on Power Delivery,* vol. 18, pp. 201-206, 2003.

[16] J. Beerten and R. Belmans, "Development of an open source power flow software for high voltage direct current grids and hybrid AC/DC systems: MATACDC," *IET Generation, Transmission & Distribution,* vol. 9, pp. 966-974, 2015.

Yanbo Che was born in Shandong, China. He received his B.S. degree form Zhejiang University, Hangzhou, China, in 1993. He received his M.S. and Ph.D. degree from Tianjin University, Tianjin, China, in 1996 and 2002, respectively. Since 1996, he has been engaged in teaching and scientific research of power electronic technology and power systems. He is presently an Associate Professor in the School of Electrical and information Engineering at Tianjin University. His current research interests include power electronics, renewable energy resources and micro-grids

Jinhuan Zhou received her B.S. degree from the University of Electronic Science and Technology of China, Chengdu, China, in 2016. Since September 2016, she has been working toward his M.S. degree at Tianjin University, Tianjin, China. Her current research interests include power electronics, HVDC transmission system control and renewable energy resources.

Wenxun Li received his B.S. degree from the China Agricultural University, Beijing, China, in 2015. Since September 2015, he has been working toward his M.S. degree at Tianjin University, Tianjin, China. His current research interests include power electronics and renewable energy resources.

Jiebei Zhu received the B.S. degree in micro-electronics from Nankai University, Tianjin, China, in 2008, and the M.Sc. and Ph.D. degrees in electronicand electrical engineering from the University of Strathclyde, Glasgow, U.K., in 2009 and 2013, respectively. From 2013, he acts as a Senior Power System Engineer and Innovation Project Manager with National Grid Plc. of the GB transmission system operator. His research interests involve with HVDC transmission system control, renewable energy systems, and energy storage technolgies. Dr. Zhu was awarded with the license of "Chartered Engineer" by UK Engineering Council and IET.

Chao Hong is a Senior Power System Engineer with the Electric Power Research Institute of China Southern Power Grid (CSG). His current research interests are in the areas of power system dynamics and control, and power system planning.